Journal of Applied Geophysics 162 (2019) 164–173

Contents lists available at ScienceDirect

Journal of Applied Geophysics

journal homepage: www.elsevier.com/locate/jappgeo

Hydrogeopysical characterization of the Haby Crossing fault, San Antonio, Texas, USA

Mustafa Saribudak *, Alf Hawkins

Environmental Geophysics Associates, 2000 Cullen Avenue, Suite 7, Austin, TX 78757, United States

ARTICLE INFO

Article history:
Received 5 October 2018
Received in revised form 17 January 2019
Accepted 19 January 2019
Available online 26 January 2019

Article impact statement

The Haby Crossing fault is considered a barrier to groundwater flow because of the large amount of displacement along the fault. The displacement of the fault has been estimated in the past by comparison of nearby boreholes and from geologic mapping. This study, for the first time, provides geophysical data to enhance the hydrogeologic understanding of the fault and fault zone deformation, its vertical and horizontal extension, fault zone deformation and its karstic features. Furthermore, the boundary of Edwards and the underlying Trinity Aquifer, was also mapped for the first time using the resistivity imaging method.

Keywords:
Geophysics
Edwards Aquifer
Balcones Fault Zone
Haby Crossing Fault

ABSTRACT

Regionally, the Haby Crossing fault is characterized as a lateral barrier to groundwater flow between the Edwards aquifer recharge zone and the confined portion of the Edwards aquifer. Results from this hydrogeophysical investigation demonstrate that karstification along the fault plane created conduits for preferential lateral flow between the Edwards and the juxtaposed Trinity aquifers which has previously not been considered in groundwater flowpath models. Two-dimensional images of electrical resistivity tomography, self-potential (SP), magnetic and conductivity (EM31) data were used to map the hydrogeologic and structural features within the study area. The contact between the Edwards and the Trinity aquifers is located on the upthrown side of the Haby Crossing fault. The resistivity data displays that the Trinity aquifer appears to be folded upwards near the fault. Further away from the fault, in the northwest direction, the data indicate that the boundary is closer to horizontal and is at a depth of approximately 75 m.

Magnetic and ground conductivity data confirm the locations of the structural features. The fault zone contains fault-related folding, faulting, and tilting as evidenced on each of the profiles. The Haby Crossing fault is a low resistivity feature indicating a high clay content in the brecciated fault material. SP anomaly types mapped vary from m-shaped to sombrero, positive, and negative, which probably indicate changes in the geometry of the karstic features as well as variations in ground-water flow conditions. These observations suggests that the Haby Crossing fault zone and its immediate area could be permeable enough to allow ground-water flow along the fault planes.

Location of karstic features, such as caves, voids or sinkholes determined by this study may identify areas of groundwater communication between the Trinity and Edwards aquifers. The results can aid in choosing an area where groundwater tracer studies can be performed to better understand the groundwater flow paths and cross aquifer communication.

1. Introduction

The karstic Edwards and Trinity aquifers are the primary sources of water for south-central Texas, including the city of San Antonio. Lithology of the Edwards aquifer is composed of mudstone to boundstone, dolomitic limestone, evaporate, and argillaceous limestone. The Trinity aquifer, which underlies the Edwards aquifer, consists of alternating layers of medium-bedded limestone and argillaceous limestone (Lambert et al., 2000). The Haby Crossing fault (HCF) is in Medina County, Texas and is located within the San Antonio segment of the Balcones Fault Zone (BFZ), which is a 25- to 30- km –wide en echelon system of mostly south-dipping normal faults that formed during the middle to late Tertiary (Fig. 1; Modified from Small and Clark, 2000). The Edwards aquifer is formed within the Edwards Group within the study area and is formed by a series of karstic limestone formations (Clark et al., 2013). Underlying the Edwards aquifer is the Trinity aquifer, which is similar to the Edwards, is formed within a series of karstic carbonate formations (Clark et al., 2013). Karst aquifers are characterized by a network of conduits and caves formed by chemical dissolution, allowing for rapid and often turbulent water flow.

The Haby Crossing fault is a long-continuous fault with significant offset (90 m) that extends from southern Hays County through central Medina County (Stein and Ozuna, 1996; Small and Clark, 2000; Lambert et al., 2000). The fault has been interpreted as a barrier fault to groundwater flow from central Medina County to southern Hays County (Maclay

* Corresponding author.
E-mail address: ega@pdq.net (M. Saribudak).

https://doi.org/10.1016/j.jappgeo.2019.01.009
0926-9851/

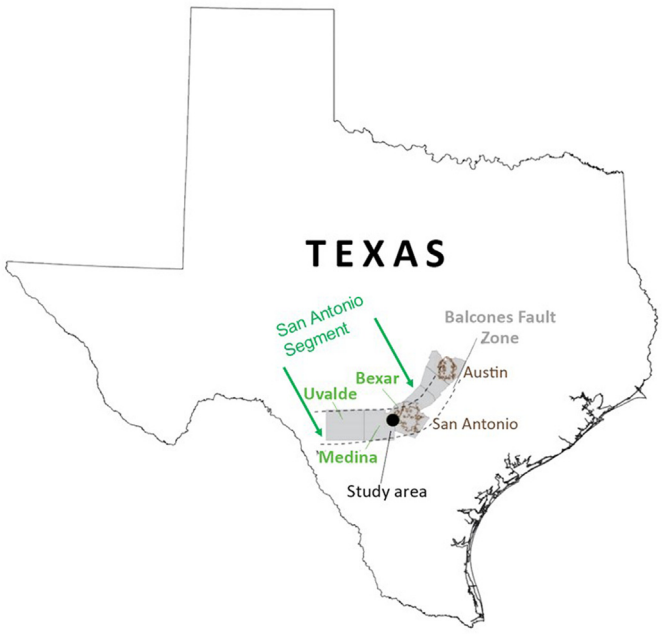

Fig. 1. Texas map showing the location of the Balcones Fault Zone, the study area and neighboring counties. The gray-shaded area corresponds to the Edwards aquifer, which is underlain by the Trinity aquifer. Note that the study area is in the north-east part of Medina County, which neighbors Bexar County from the east.

and Land, 1988; Lindgren et al., 2004). This characterization appears justified at least at the two ends of the fault (Liu et al., 2017); but there is no subsurface data available to make similar interpretation along the central segment of the fault, which includes the study area.

There have been three major geophysical surveys near the current study area by the United States Geological Survey (USGS): 1) Ground geophysical survey results over the northeastern Bexar county (Shah et al., 2008) were used to improve the geological mapping and the hydrostratigraphy by providing average resistivity values for each hydrostratigraphy unit of the Edwards Aquifer; 2) results of geophysical studies (a helicopter electro-magnetic and two-dimensional, direct current (2D-DC) resistivity surveys) over the Camp Bullis Training Site in Bexar County correlated well with the mapped geologic outcrops. Results of the investigation identified zones of high density karst features and characterized karstic voids, including caves (Gary et al., 2013); 3) ground and airborne geophysical surveys conducted over western Medina and Uvalde Counties (Blome et al., 2008) have provided critical data on fault morphology and displacement, potential areas of karst development, and the geohydrologic properties of water-bearing units.

This study expands upon the work done by Saribudak et al. (2010) over the Haby Crossing fault. In this previous study we conducted resistivity imaging, self-potential (SP) magnetics and conductivity surveys to investigate the fault. Each geophysical survey characterized the fault and provided additional information. However, results did not reveal any information on the geologic contact between the Edwards and Trinity aquifers.

In the year of 2017 and 2018, we collected more data by conducting geophysical surveys at three more locations, which are located to the west of the previous location, and are spaced in the strike direction of the fault. We used resistivity imaging and SP techniques for these surveys. The reason we used more than one technique because integrated geophysical methods provide more reliable results. Thus, the goal of this study was to characterize the signature of the fault anomalies for each geophysical method and enhance our understanding of the fault zone deformation, and hydrogeological setting, and map the boundary between Edwards and Trinity aquifers.

2. Hydrogeologic setting

Movement of water in the Edwards aquifer, and to a lesser extent in the Trinity aquifer, is controlled by an extensive fault system known as the Balcones fault zone (BFZ). The BFZ consists of a dense series of near parallel, primarily northeast-trending faults that commonly are normal, high-angle structures with the downthrown side to the southeast (Maclay, 1995). These faults can form barriers or conduits to flow. The degree of hydraulic connection between two adjacent fault blocks depends on the amount of vertical displacement (or throw) on the fault and the proportion of total thickness of porous, permeable units of the Edwards aquifer juxtaposed against porous, permeable units of the Trinity aquifer. Maclay and Land (1988) define flow-barrier faults as faults that have a vertical displacement of greater than 50% of the total thickness of the Edwards aquifer.

The Edwards aquifer in the BFZ is one of the most permeable and productive carbonate aquifers in the USA, consisting of extensively faulted, fractured, and cavernous limestone and dolomite (Maclay, 1995). The Edwards aquifer comprises the Kainer and Person Formations of the Edwards Group, plus the overlying Georgetown Formation (Lambert et al., 2000; Small and Clark, 2000; Small et al., 1996).

The Edwards Aquifer is between 91 and 213 m thick. It includes the Edwards Group and other associated limestone and is underlain by the upper member of the Glen Rose Limestone, Upper zone of the Trinity aquifer, which consists of hard limestone strata alternating with marl or marly limestone. The upper member of the Glen Rose Limestone underlying the Edwards Group has historically been interpreted as a confining zone (Rose, 1972; Edwards Aquifer website: http://www.edwardsaquifer.net/geology.html). However, recent awareness of a significant connection between the Edwards and Trinity aquifers has resulted in a number of hydrogeologic investigations documenting that they actually operate as a single system in some locations and under certain circumstances (Clark, 2003; Clark et al., 2009; Smith and Hunt, 2010; Wong et al., 2014; Hunt et al., 2015; Clark et al., 2016).

The geological map of the Haby fault and its hydrogeologic section A-A', which is approximately located about 6 km to the geophysical study area, is provided in Fig. 2 (Lambert et al., 2000).

The Edwards Group in this area primarily consist of the basal nodular, dolomitic, Kirschberg evaporite, and grainstone members of the Kainer Formation, with caps of the regional dense member and the leached and collapsed members, undivided, of the Person Formation. The large vertical displacement on the Haby Crossing fault completely offsets the Edwards Group units on the upthrown side against the younger confining units (see cross-section A-A' and geological legend in Fig. 2). The thickness of the dolomitic member and the underlying basal nodular member from the surface is about 70 m (Fig. 2). Thus the depth to the geologic contact between the Edwards Group and the underlying Trinity Group (upper member of the Glen Rose member) is approximately 70 m from the surface on the upthrown side of the fault. The contact is one of the targets of the current geophysical study.

However, in the study area the dolomitic member of the Edwards Group is exposed on the upthrown side of the fault (Lambert et al., 2000; Small and Clark, 2000). Surficial deposits cover the downthrown side of the fault hiding outcrops of the younger rocks of the Upper confining units.

Ferrill and Morris (2008) showed that fault zone character in the Balcones fault system are strongly influenced by mechanical stratigraphy (mechanical strength of rocks). Faulting in the massive, clay poor limestones of the Edwards Group is characterized by steep fault dips, little or no clay smear, little or no bed tilting, small-displacement normal faults near larger displacement faults, and common cataclasis in fault rocks. In the overlying shale-rich Del Rio, Buda, and Eagle Ford, faulting is characterized by moderate to steep fault dips, clay smear developed from the Eagle Ford and Del Rio, monoclinal folding, and bed tilting (Ferrill and Morris, 2008).

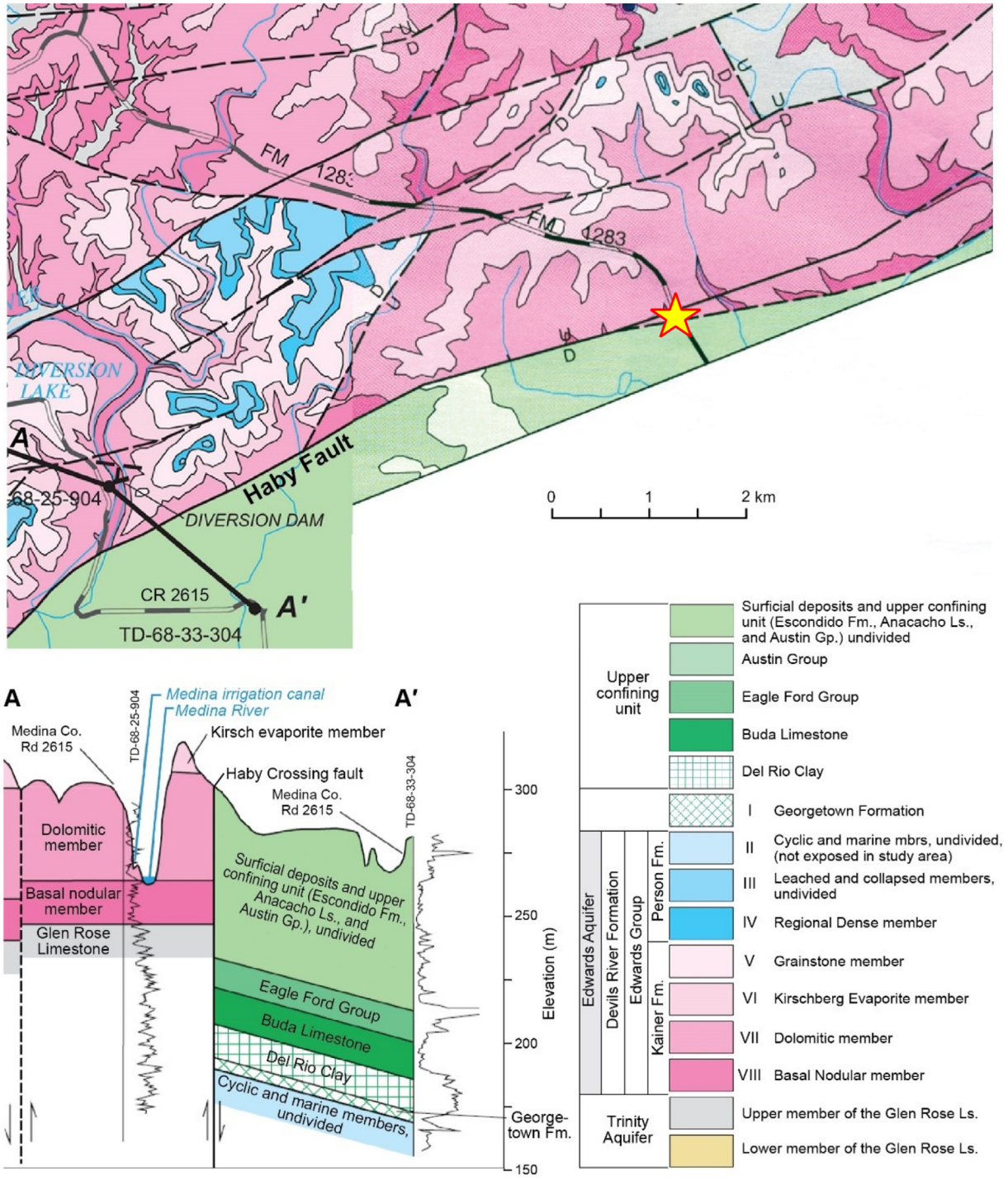

Fig. 2. Geological map above) and eight of Hydrostratigraphic and the Upper confining units (below) of the study area (Lambert et al., 2000). The symbol red/yellow star (★) indicates the geophysical study area across the Haby Crossing fault. (For interpretation of the references to color in this figure legend, the reader is referred to the web version of this article.)

Faulting in the underlying, more clay-rich, and well-bedded Glen Rose is characterized by small-displacement faults that have gentler dips than in the Edwards. Large-displacement faults have moderate to steep dips, clay smear is locally present, derived from clay shale beds in Glen Rose, monoclonal folding and bed tilting are common adjacent to main-displacement fault surfaces (Ferrill and Morris, 2008).

The Haby Crossing fault juxtaposes all three rock types above, which are categorized as: 1) low competent (Glen Rose), 2) high competent (Edwards), 3) and incompetent (Del Rio, Buda, Eagle Ford Formations, and younger units). For this reason, the interpretation of the geophysical data, specifically the resistivity data, will be interpreted in the light of the above-mentioned study.

3. Hydrogeophysical investigation of the Haby Crossing fault

The discussion of the geophysical data in this paper includes the previous study, which is a multi-method geophysical survey conducted along one profile (P1) for the City Public Service (CPS) Energy's proposed transmission line route (Saribudak et al., 2010). The purpose of the survey was to image the subsurface to a depth of about 40 m

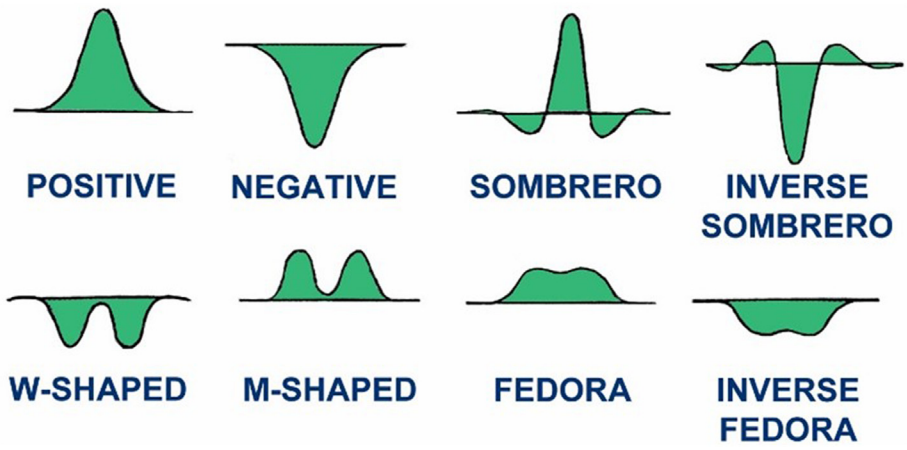

Fig 3. Typical SP anomaly types commonly observed over caves and karst springs. The changing shapes are attributed to the changes in the geometry of the caves and as well as variations in flow conditions (Lange, 1999).

below, to map geologic and structural features, and to identify karst features across the Haby Crossing fault.

In this study, three additional profiles were surveyed. Only resistivity imaging and self potential (SP) data were collected. The locations of these geophysical profiles and the previous profile, are shown with different colors in Fig. 3. The first profile (P1) is depicted in yellow. The other two geophysical profiles (P2 and P3) (red and light blue colors) were obtained from the western ditch. One additional geophysical profile (orange in color) was surveyed in the eastern ditch adjacent to FM 1283 Road. All profiles traverse the fault; but the extension of profile P4 was limited across the fault because of a driveway which intersected the profile.

4. Hydrogeophysical methods

Integrated geophysical methods can provide new insights into the karstic features and faults. There has been some geophysical studies published, which indicate the utilization of these methods across the Edwards Aquifer (Connor and Sandberg, 2001; Saribudak et al., 2012; Saribudak et al., 2013; Saribudak, 2016; Saribudak and Hauwert, 2017) and other locations (e.g. Carpenter, 1998; Ahmed and Carpenter, 2003; Dobecki and Church, 2006).

4.1. Electrical resistivity tomography

The 2D resistivity method images the subsurface by applying a constant current in the ground through two current electrodes and measuring the resulting voltage differences at two potential electrodes some distance away. An apparent resistivity value is the product of the measured resistance and a geometric correction for a given electrode array. Resistivity values (ohm-m) are highly affected by several variables, including the presence of water or moisture, and the amount and distribution of pore space in the material, and temperature (Rucker and Glaser, 2015). The Advanced Geosciences, Inc. (AGI) SuperSting R1 was used with a dipole-dipole array with a 6.1 m (20 ft) electrode spacing using a roll-along mode for the first profile in this study. The R8 resistivity meter was later used with a mixed electrode array (Schlumberger and dipole-dipole) using 56 electrodes for profiles 2, 3 and 4. The electrode spacing for profiles 2, 3 and 4 was 6.1 m (20 ft), 10 m (33 ft), and 6.1 m (20 ft) respectively. The mixed array is relatively sensitive to horizontal and vertical changes in the subsurface (compared to other arrays). We used Advance Geoscience's EarthImager 2D software to provide a 2-D electrical image of the near-surface geology. Contact resistance test for each profile was performed before the data collection. Contact resistance measures the resistance to current flow at electrodes caused by imperfect electrical contact with the earth. Poor data quality or anomalous data can result from high or highly variable electrode contact resistance along a profile. To decrease the effect of contact resistance along each profile saltwater solution was added at ~~to~~ each electrode before the contact resistance test was performed.

Contact resistance values along profile P1 varied between 60 and 300 Ohm over the downthrown section of the fault whereas resistance increased to as high as 3000 Ohm on the upthrown side where the high resistive dolomitic rocks are exposed. The remaining three profiles (P2, P3 and P4) resistance values ranged between 200 and 550 Ohm because the ground is covered with several inches of soil.

AGI EarthImager 2D is a two-dimensional inversion modeling software for resistivity imaging (EarthImager 2D Manual, 2002–2014). It interprets data collected by the resistivity meter. The data set collected is processed into a 2D cross-section of the earth using a smooth-model inversion method. The inversion values of RMS and L2 parameters were used to judge the quality of the resistivity data. The quality of the inverted resistivity data ranged fair to good overall because RMS and L2 values varied from 5 to 22, and 1 to 13, respectively. The noise filter for the software was automatically set for removing the negative resistivity values. The highly resistive dolomitic rock (a member of Kainer Formation), which is exposed on the upthrown side of the fault, resulted in noisy data causing RMS value up to 22 for profile P1. As a result of noisy data, the option to "Suppress Noisy Data" was used in the inversion software of EarthImager 2D to minimize the effects. There were not any cultural sources of interference along the P1 to affect the data. The remaining three profiles (P2 through P4) resulted in little to no noise even with passing traffic and power lines nearby.

4.2. Self potential (SP)

Self-potential (SP) is the naturally occurring electrical potential of the earth resulting from geologic, geochemical, and hydrologic interactions which cause electric potentials to exist in the earth in the vicinity of the measurement point (Lange and Kilty, 1991; Lange, 1999; Vichabian and Morgan, 2002; Revil and Jardani, 2013). One of the primary sources of self-potential signals is fluid flow in porous media, such as groundwater flow or seepage through a dam or spring (Minsley et al., 2011; Saribudak and Hauwert, 2017). An excess positive charge that develops near grain surfaces in saturated porous geologic media is transported along with the fluid, creating a streaming current density. This subsurface electrokinetic phenomenon generates a balancing conduction current density, which flows through the earth resistivity structure and is manifested as the measurable self-potential on the earth surface (Minsley et al., 2011, Morgan et al., 1989, Revil et al., 1999).

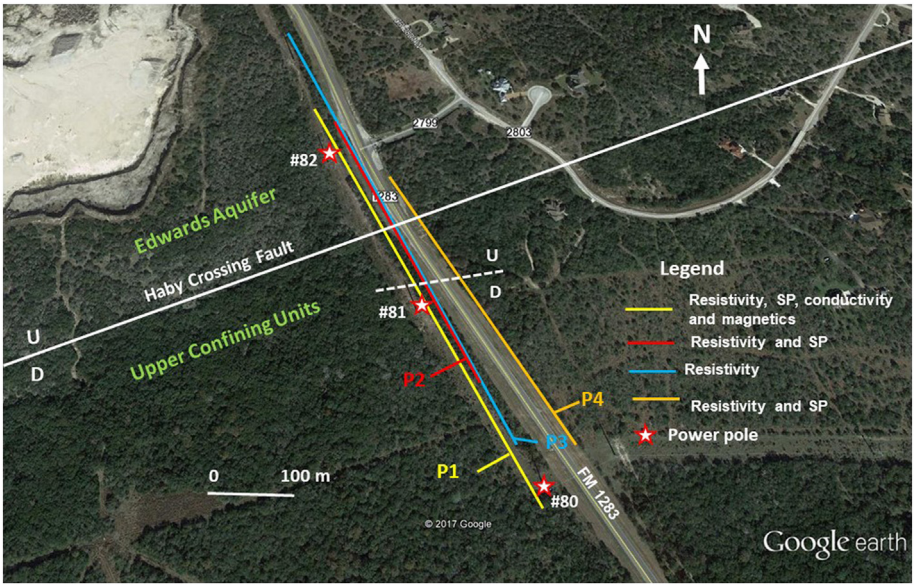

Fig 4. Site map indicating the location of the Haby Crossing fault, geophysical profiles, and location of transmission poles (80 through 82) for reference purposes (see text for explanation).

Natural electrical currents occur everywhere in the subsurface. Slowly varying direct currents (D.C.) give rise to a surface distribution of natural potentials due to the flow of groundwater within permeable materials, which help locate karstic features, such as caves and sinkholes (Lange and Kilty, 1991, Lange, 1999, Vichabian and Morgan, 2002, and Saribudak and Hauwert, 2017; see Fig. 4). Differences of potential are most commonly in the millivolts range and can be detected using a pair of non-polarizing copper sulfate electrodes and a sensitive measuring device (i.e. a voltmeter or potentiometer). It should be noted that SP measurements made on the surface are the product of electrical current due to groundwater flow and the subsurface resistivity structure (Atangana et al., 2015).

SP geophysical surveys measure the potential difference between any two points on the ground produced by the small, naturally produced currents that occur beneath the Earth's surface. The SP method is passive, non-intrusive and does not require the application of an electric current. Small potentials of the order of a few millivolts are produced by two electrolytic solutions of differing concentrations that are in direct contact, and by the flow of groundwater through porous materials (streaming potential). Slowly varying direct currents (D.C.) give rise to a surface distribution of natural potentials due to the flow of groundwater within permeable materials, which help locate karstic features, such as caves and sinkholes (Lange and Kilty, 1991, Lange, 1999, Vichabian and Morgan, 2002, Saribudak et al., 2010; and Saribudak and Hauwert, 2017).

A SP survey involves utilizing a base station in conjunction with a roving electrode. The base station is connected to the roving station on a reel. A voltmeter is used to measure the subsurface electrical field in millivolt (mV) between the base station and the roving electrodes. The accuracy of the voltmeter was 0.1 mV. SP data collected in varying station spacing of 4.5, 6, and 9 m. These data points are shown as filled-circles on SP profiles.

4.3. Conductivity data

The electro-magnetic (EM) method provides a rapid means of measuring the electrical conductivity of subsurface materials including soil, rock, buried wastes and karstic features. A Geonics EM-31 conductivity instrument was used for this survey. The EM-31 unit contains an intercoil spacing of 3.6 m (12 ft) and has an effective depth exploration of up to 6 m (20 ft), depending on the conductivity of the subsurface soil and/or rocks. It measures conductivity contrast of the subsurface geology in milliSiemens/m (mS/m). EM 31 data can aid in the characterization of the following: Paleochannels (buried streams), faults, and fractures; karstic features, such as caves and sinkholes; lateral extent of buried wastes, landfills, metal objects and/or trench materials; and contaminant plumes and groundwater migration paths (McNeill, 1980, Carpenter, 1998, Saribudak, 2016, and Geonics, Inc., website www.geonics.com). The EM-31 data was collected only along profile P1. The collection rate of the conductivity data was such that the spacing between the data points was about 0.5 m along the profile.

4.4. Magnetic data

Instrumentation used for the magnetic survey was a G-858 cesium magnetometer. It measures Earth's magnetic field in nanoTesla (nT), and thus can detect ores, faults, fractures, caves containing ferrous minerals, etc., in the subsurface (Azate et al., 1990, Blakely, 1995, Hinze, 1990, Saribudak et al., 2018). The magnetic data was collected in a continuous mode. The collection rate of the magnetic data was such that the spacing between the data points was less than 0.2 m along the magnetic profile. The instruments sensitivity is approximately 0.1 nT.

5. Hydrogeophysical characterization of the Haby Crossing fault

5.1. Profile one

Resistivity imaging, SP, conductivity, and magnetic surveys were performed across the Haby Crossing fault along P1 (Fig. 5). A magnetic base station in the middle of the site was established, which was visited before and after the magnetic survey, in order to correct for the earth's magnetic field diurnal variations. The magnetic survey lasted 16 min. We did not observed any magnetic drift, thus no correction was applied to the data. Roll-along resistivity data was collected using two resistivity cables, each cable having 14 electrodes with 20-ft electrode spacing. After the initial section of resistivity data was collected, the first cable of 14 electrodes was moved

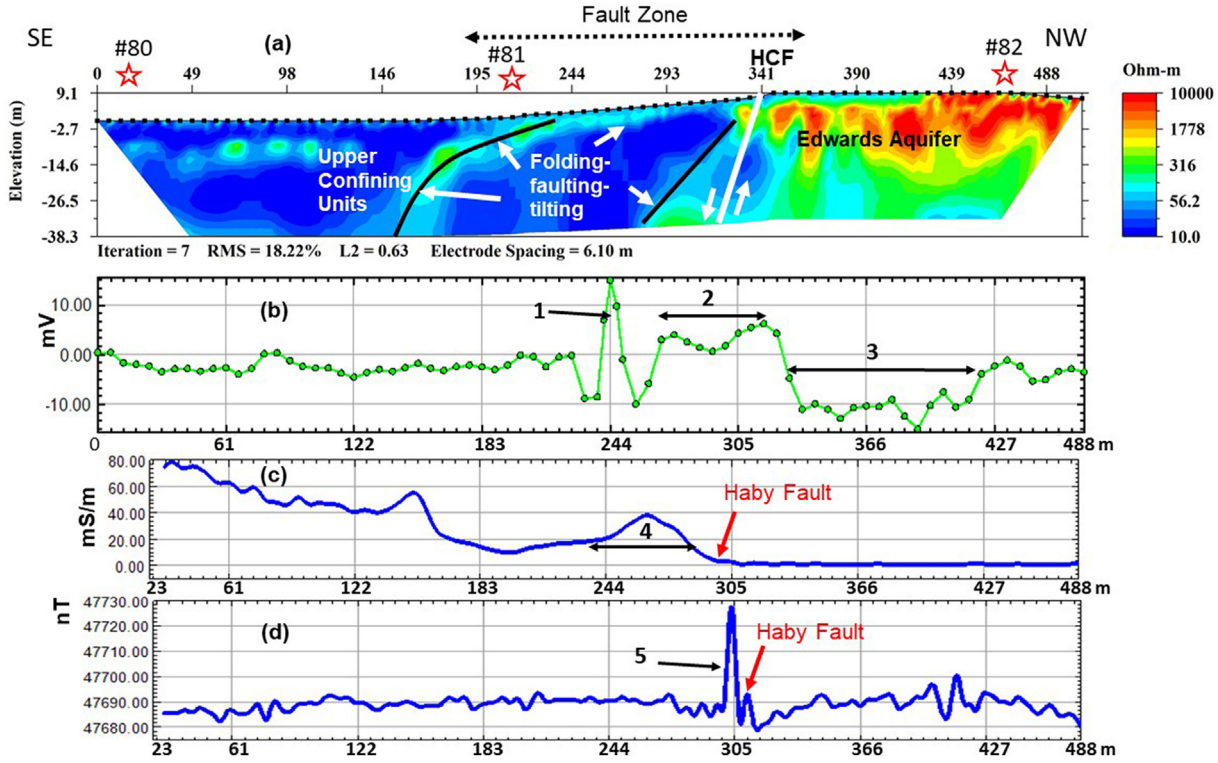

Fig. 5. Resistivity imaging (a), SP (b), EM31 conductivity (c), and magnetic (d) data along profile P1 across the HCF. CPS Energy's transmission pole locations (#80 through #82) are shown for reference purposes.

ahead of the survey line. This process was continued until all data along the desired length were collected.

The resistivity imaging data shows a large fault zone, rock units, and CPS Energy's transmission poles (#80 through #82) along profiles for reference purposes (Fig. 5a).

The resistivity values of geological units across the Haby Crossing fault, which juxtaposes the Edwards aquifer (dolomitic member of Kainer Formation) with the Upper confining units (surficial deposits, Escondido Formation, Anacacho Limestone, and Austin Group and other older units) vary between 10 and 10,000 Ohm-m. The location of Haby Crossing fault is shown with a dip of 70° (Written communication with Ronald McGinnis of SWRI, 2018). The maximum depth of exploration of resistivity data is about 45 m. The resistivity data displays a fault zone with a width of about 160 m.

It should be noted that the contact between the high (red in color) and moderate resistivity (green in color) limestone layers of Kainer Formation have a very irregular geometry, which may be caused by the tectonic and/or weathering activity (Epi-karst). There is a large low- resistivity area to the immediate southeast of the Haby Crossing fault, which might be the result of fault related folding (Written

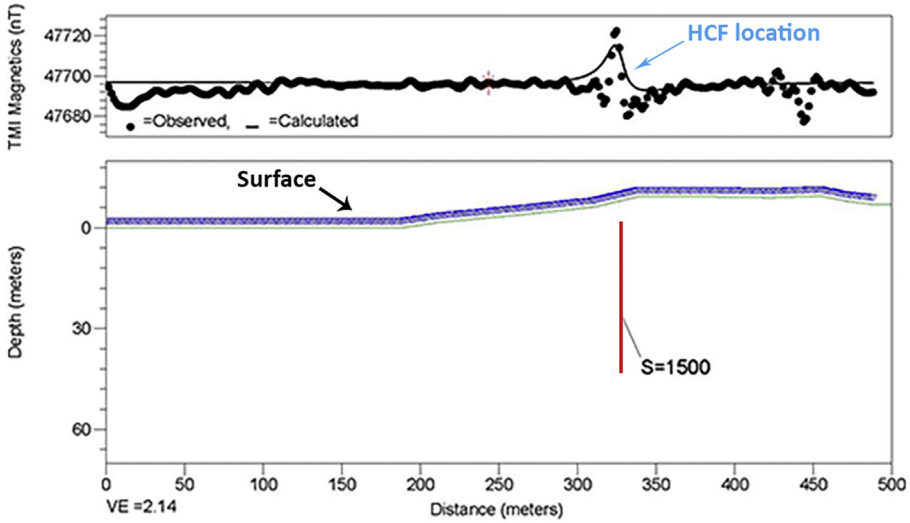

Fig. 6. Modeling of magnetic data. The blue arrow indicates the Haby fault location. The blue arrow on the observed magnetic data shows the location of the HCF. The high magnetic anomaly is interpreted to be the narrow zone of anomalously magnetized material (red line) along the fault. The magnetic data was modeled using a 10-m lowpass-filtered signal. (For interpretation of the references to color in this figure legend, the reader is referred to the web version of this article.)

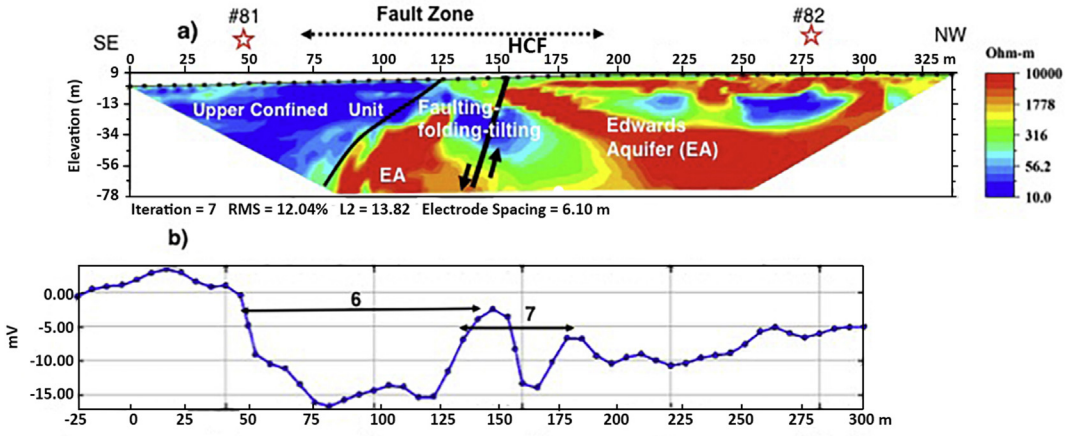

Fig. 7. Resistivity tomography (a) and SP (b) data along profile P2 across the Haby Crossing fault (HFC).

communication with Ronald McGinnis of SWRI, 2018). This zone of low resistivity may also be interpreted as fault breccia (pulverized rock resulting from friction associated with fault movement) or clay filling along the fault, which if present could impede local ground-water flow (Smith et al., 2005).

The SP data collected along P1 indicates anomalies which are interpreted as karst features (SP anomalies #1 through #3) within the fault zone (Fig. 5b). Anomalies 1 through 3 are categorized as positive, m-shaped, and negative, respectively (see Fig. 4).

Note that the SP values drop steeply across the Haby Crossing fault forming a negative anomaly (#3). The negative SP anomaly are often encountered over recharge areas of the karstic terrain of the Edwards Aquifer (Saribudak et al., 2013; Saribudak, 2016). This is due to fact that the infiltrating surface water creates negative charges near the surface and positive charges in the direction of the water movement.

The EM31 conductivity data is presented in Fig. 5c. The conductivity data marks the location of the Haby Crossing fault well. The conductivity data also indicates a high conductivity anomaly, which is marked as #4 on the profile, across the fault zone, which correlates well with the low resistivity zone in the 2D resistivity data, and the location of #1 and #2 SP anomalies.

There is a significant high magnetic anomaly where the fault is located (Fig. 5d). This anomaly is a short-wavelength, which has a width of 5 m. and its magnitude is 47,730 nT. The source for the magnetic anomaly could be due to a localized ferrous mineralization across the fault plane. It should be noted that the SP anomaly #2 correlates well with the location of the magnetic anomaly suggesting that the magnetic mineralization could be within a karstic feature as well, such as cave.

In order to quantify the magnetic source, a model of the magnetic data was created using 2D forward modeling software (Geosoft Oasis Montaj GMSYS2D). The magnetic susceptibility of the model was iteratively modified until the computed response matched the observed magnetic anomaly (Fig. 6).

A model of the shallow fault zone was created using relatively high magnetic susceptibility (1500 micro-CGS) across a very narrow feature. The geometry of the modeled magnetic response of the fault zone, which is non-unique, indicates that this is a reasonable explanation of a possible source of the observed magnetic anomaly near the Haby Crossing fault. The high magnetic zone is 1.4 m wide and extends from 7 m below the topographic surface to 50 m below the topographic surface.

In summary, four different geophysical methods provide significant, otherwise unavailable, information on the location of potential karstic features, ferrous mineralization, and fault characterization across the Haby Crossing fault.

5.2. Profile two

P2 was located 60 ft to the west of P1 (Fig. 3). Only the resistivity and SP surveys were performed along this profile. The resistivity data were collected using four resistivity cables, each having 6.1 m electrode spacing with 56 electrodes. The maximum depth penetration was about 80 m. The color range of the resistivity section is fixed between 10 and 10,000 Ohm-m, as profile P1, so that a correlation can be made between resistivity profiles.

The resistivity data shows similar anomalies as in P1 (Fig. 7a). The fault zone width is about 130 m, but it narrows towards the Haby Crossing fault. The fault zone contains a significant size of a resistive block in the downthrown side of the Haby Crossing fault. The resistive block appears to be detached from the Edwards aquifer. The upper confining units are shown with the low resistivity values of 10 Ohm-m (dark blue color) on the southeast side of the fault. The area of upper confining unit rocks and the Edwards aquifer indicate fault-related folding, faulting and tilting within the fault zone. The low resistivity area within the fault zone is probably caused by fault breccia (Fig. 7a).

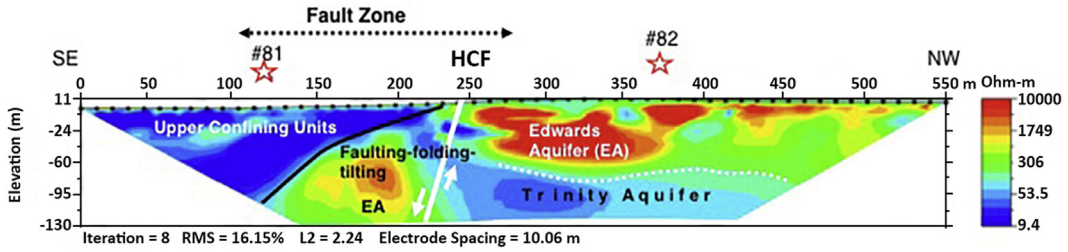

Fig. 8. Resistivity imaging data along profile P3 across the Haby Crossing fault (HCF).

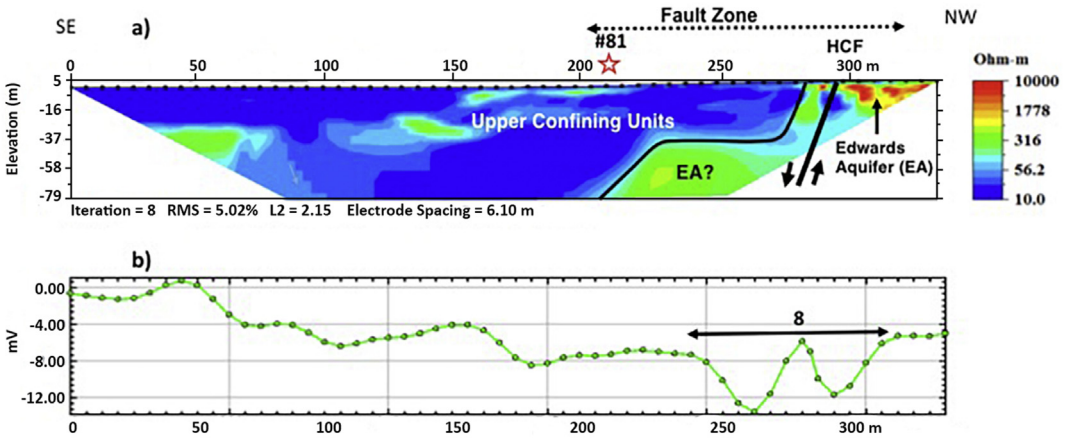

Fig. 9. Resistivity imaging (a) and SP (b) data along profile P4 across the Haby Crossing fault (HCF).

It should be noted that the maximum depth exploration is about 90 m and the upthrown side of the Haby Crossing fault is dominantly Edwards aquifer rocks. The resistivity data does not indicate the presence of the Trinity aquifer underlying the Edwards aquifer.

The SP data collected along P2 indicates two significant anomalies interpreted as karst features. The anomalies are marked with numbers as 6 and 7 on Fig. 7b. Anomalies #6 and #7 are categorized as negative and m-shaped anomalies.

5.3. Profile three

One of the goals of this study was to map the boundary between the Edwards aquifer and the underlying units of Trinity aquifer. The resistivity data along profiles P1 and P2 did not reveal any such ~~a~~ boundary. The lack of data indicating the boundary between the Edwards and Trinity aquifers prompted the collection of more resistivity data with a larger electrode spacing to explore deeper depths across the fault. Examining deeper depths a new resistivity profile P3 was surveyed using 56 electrodes with a 10 m electrode spacing next to P2 (see profile location in Fig. 3). The length of the profile is about 550 m, which yielded a maximum exploration depth of 140 m (Fig. 8).

There is a discernible boundary at about 75 m between high (red in color) to low (blue in color) resistivity areas on the upthrown side of the Haby Crossing fault. The change is consistent with the contact of the Edwards aquifer (dolomitic member) and Trinity aquifer (Glen Rose Formation), and is associated with the change in lithology going from a pure limestone to an argillaceous limestone (Allan Clark of USGS, Pers. Comm., 2017). There are water wells in the northern vicinity of the Haby Crossing fault that produce from the Trinity aquifer. The depth of the producing zone closely matches with depth of the Trinity aquifer obtained from this resistivity survey (Taylor Bruecher of Edwards Aquifer Authority, Pers. Comm., 2017). In addition, the estimated thickness of the Edwards aquifer's thickness in the vicinity of the study area (Lambert et al., 2000) is about 70 m, which correlates well with the resistivity data.

The width of the fault zone is about 150 m, but it narrows towards the Haby Crossing fault. The fault zone displays faults, fault-related folding and tilting. The fault zone also contains a high-resistivity block of a significant size in the downthrown section, as in profile P2.

5.4. Profile four

P4 was conducted in the western ditch along FM 1283 parallel to other profiles (Fig. 3). Both resistivity and SP surveys were conducted along the profile. In this survey, 56 electrodes were used with an electrode spacing of 6.1 m. The depth of exploration was about 85 m. This profile was terminated short because of the presence of a driveway in the northern part of the Haby Crossing fault (see Fig. 3).

Fig. 9a shows the resistivity imaging data collected along profile P4. The Haby Crossing fault juxtaposes the upper confining units with the dolomitic member of the Edwards aquifer (Fig. 9a). Majority of the resistivity section is covered with the upper confining units, which are shown with the blue color. The width of the fault zone is about 130 m, which is correlative with other resistivity profiles, and narrows down towards the HCF. The fault zone contains, faulting related folding, faulting and tilting of the rocks as shown on other profiles.

The SP data is provided in Fig. 9b, which indicates a significant sombrero-type anomaly in the vicinity of the Haby Crossing fault. The source for this anomaly is probably karstic. The SP profile also indicates an increasing gradient in the southeast direction. This gradient is not observed on previous two SP profiles, and its reason is unknown.

6. Summary and conclusion

The Haby Crossing fault is one of the most significant faults in the Balcones Fault Zone, located in Medina County, Texas. Karstic features, fault signatures, fault deformation, and the buried Edwards/ Trinity contact were analyzed using geophysical techniques, which consisted of resistivity imaging, self-potential (SP), magnetics and conductivity. The fault location was detected by each geophysical method. All four resistivity profiles display a large fault zone whose width varies between 130 and 160 m. The fault zone on each profile contains fault-related folding (monoclinal folding), faulting and tilting.

Faulting in the underlying, more clay-rich, and well-bedded Glen Rose is characterized by small-displacement faults that have gentler dips than in the Edwards. Large-displacement faults have moderate to steep dips, clay smear is locally present, derived from clay shale beds in Glen Rose, monoclonal folding and bed tilting are common adjacent to main-displacement fault surfaces (Ferrill and Morris, 2008).

The resistivity data on each profile also indicates a low resistivity area in the fault deformation zone, which is probably caused by clay and fault breccia along the fault plane. In addition, two adjacent resistivity profiles (P2 and P3) with different profile spacing display a high resistivity block displaced from the Edwards aquifer rocks in the downthrown part of the Haby Crossing fault.

The SP data indicate anomalies that may indicate the presence of karst features within this fault zone. SP anomaly types mapped vary from m-shaped to sombrero, positive, and negative, which probably indicate changes in the geometry of the karstic features as well as variations in ground-water flow conditions. These observations suggests that the Haby Crossing fault zone and its immediate area could be permeable enough to allow ground-water flow along the fault planes.

The conductivity and magnetic profiles mapped the location of the Haby Crossing fault and correlate well with the resistivity and SP data. In addition, magnetic data indicated a high anomaly near the fault, which could be due to the magnetic mineralization across the fault plane or presence of karstic features embedded with magnetic minerals.

The resistivity imaging data with the largest profile spacing (10 m) along the western ditch of FM 1283 Road (profile P3) indicates the geological contact between the Edwards and the Trinity aquifers on the upthrown side of the Haby Crossing fault. The Trinity aquifer units appear to be folded upwards near the fault. However, away from the fault, in the northwest direction, the resistivity data shows that the boundary is smoother and is about 75 m deep, and appears to be horizontal. The estimated thickness of the Edwards Aquifer's thickness in the vicinity of the study area is about 70 m, which correlates very well with results of resistivity data.

In conclusion, the understanding of geologic structure is a key component to understanding groundwater flow paths within the Edwards aquifer recharge and confined zones. This geophysical study was performed in an area where little was known about the juxtaposition of the aquifer along a major fault. The possibility of conduits predicted by this study may also identify areas of groundwater communication between the Trinity and Edwards aquifers. These areas are probably the most likely places groundwater tracer studies can be performed to better understand the groundwater flow paths and areas of cross aquifer communication.

Acknowledgment

We would like to thank to students Nick Quante, John Cooper, and Tyler Mead of University of Texas San Antonio (UTSA) for their enthusiastic help in the field.

Special thanks and acknowledgment are to geologist Allan Clark of USGS of San Antonio office for his reviewing the manuscript, and providing insightful comments. His review has greatly improved the flow of the English and the content of the manuscript. We also thank Ronald McGinnis of SWRI for his encouragement for the publication of this manuscript and fruitful discussion on the mechanism of the faults within the Balcones Fault Zone. Lastly, I appreciate Michal Ruder of Wintermoon Technologies, Inc. for her help in modeling the magnetic data.

This project was borne out of personal curiosity and was financially supported by Environmental Geophysics Associates.

References

Ahmed, S., Carpenter, P.J., 2003. Geophysical response of filled sinkholes, soil pipes and associated bedrock fractures in thinly mantled karst, East-Central Illinois. Environ. Geol. 44, 705–716.

Atangana, J.Q.Y., Angue, M.A., Nyeck, B., Ndongue, C., Tchatat, J.T., 2015. Electrical characterization and mineralogical differentiation of a weathering cover in the South Cameroon Humid Intertropical zone using the self-potential method. J. Environ. Eng. Geophys. 20 (1), 57–70.

Azate, J., Flores, L., Chavez, R., Barba, L., Manzanilla, L., 1990. Magnetic prospecting for tunnels and caves in Teotihuacan, Mexico. In: Ward, S.H. (Ed.), Geotechnical and Environmental Geophysics: 1, Society Exploration Geophysicists, pp. 155–162.

Blakely, R.J., 1995. Potential Theory in Gravity and Magnetic Applications. Cambridge University Press.

Blome, C.D., Smith, B.D., Smith, D.V., Faith, J.R., Hunt, A.G., Moore, D.W., Miggins, D.P., Ozuna, G.B., Landis, G.P., 2008. Multidisciplinary Studies of the Edwards Aquifer and Adjacent Trinity Aquifer of South-Central Texas, Search and Discovery Article #80018, Adapted from Oral Presentation at AAPG Annual Convention. http://pubs.usgs.gov/fs/2006/3145.

Carpenter, P.J., 1998. Geophysical character of buried sinkholes on the Oak Ridge Reservation. Tennessee J. Environ. Eng. Geophys. 3, 133–146.

Clark, A.C., 2003. Geologic Framework and Hydrogeologic Features of the Glen Rose Limestone, Camp Bullis Training Site, Bexar County, Texas, U.S.GS Water-Resources Investigations Report 03–4081.

Clark, A.R., Blome, C.D., Faith, J.R., 2009. Map Showing Geology and Hydrostratigraphy of the Edwards Aquifer Catchment Area, Northern Bexar County, South-Central Texas, USGS Open-File Report 2009–1008.

Clark, A.K., Pedraza, D.E., Morris, R.R., 2013. Geologic Framework, Structure, and Hydrogeologic Characteristics of the Knippa Gap Area in Eastern Uvalde and Western Medina Counties, Texas, USGS Scientific Investigations Report 2013–5149.

Clark, A.K., Golab, J.A., Morris, R.R., 2016. Geologic Framework and Hydrostratigraphy of the Edwards and Trinity Aquifers within Northern Bexar and Comal Counties, Texas. USGS Scientific Investigations Map 3366.

Connor, C.B., Sandberg, S.K., 2001. Application of Integrated Geophysical Techniques to Characterize the Edwards Aquifer, Texas, STGS Bulletin, March Issue. pp. 11–25.

Dobecki, T., Church, S., 2006. Geophysical applications to detect sinkholes and ground subsidence. Leading Edge 336–341 v. 25, v.3.

EarthImager 2D Manual, 2002-2014. Resistivity and IP Inversion Software, Version 2.4.2., by Advanced Geosciences, Inc.

Ferrill, D.A., Morris, A.P., 2008. Fault zone deformation controlled by carbonate mechanical stratigraphy, Balcones Fault System, Texas. AAPG Bull. 92, 359–380.

Gary, M.O., Rucker, D.F., Smith, B.D., Smith, D.V., Befus, K., 2013. Geophysical Investigations of Edwards-Trinity Aquifer System at Multiple Scales: Interpreting Airborne and Direct Current Resistivity in Karst: 13th Sinkhole Conference, NCKRI Symposium 2. pp. 195–206.

Hinze, W.J., 1990. The role of gravity and magnetic methods in engineering and environmental studies. In: Ward, S.H. (Ed.), Geotechnical and Environmental Geophysics: 1, Society Exploration Geophysicists, pp. 75–126.

Hunt, B.B., Smith, A.B., Andrews, A., Wierman, D.A., Broun, A.S., Gary, M.O., 2015. Relay Ramp Structures and their Influence on Groundwater Flow in the Edwards and Trinity Aquifers, Hays and Travis Counties, Central Texas, 14th Sinkhole Conference.

Lambert, R.B., Grimm, K.C., Lee, R.W., 2000. Hydrogeology, Hydrologic Budget, and Water Chemistry of the Medina Lake Area, Texas, U.S. Geological Survey Water-Resources Investigations Report 00–4148.

Lange, A.L., 1999. Geophysical studies at Kartchner Caverns State Park, Arizona. J. Cave Karst Stud. 61 (2), 68–72.

Lange, A.L., Kilty, K.T., 1991. Natural potential responses of karst systems at the ground surface. Proceedings of the Third Conference on Geohydrology, Ecology and Monitoring and Management of Ground Water in Karst Terranes. National Groundwater Association, pp. 179–196.

Lindgren, R.J., Dutton, A.R., Hovorka, S.D., Worthington, S.R.H., Painter, S., 2004. Conceptualization and Simulation of the Edwards Aquifer, San Antonio Region, Texas, Scientific Investigations Report–5277.

Liu, A., Troshanov, N., Winterle, J., Zhang, A., Eason, S., 2017. Updates to the MODFLOW Groundwater Model of the San Antonio Segment of the Edwards Aquifer, Edwards Aquifer Authority Workshop, San Antonio.

Maclay, R.W., 1995. Geology and Hydrology of the Edwards Aquifer in the San Antonio Area. U.S. Geological Survey Water-Resources Investigations Report, Texas.

Maclay, R.W., Land, L.F., 1988. Simulation of Flow in the Edwards Aquifer, San Antonio Region, Texas, and Refinements of Storage and Flow Concepts: U.S. Geological Survey Report Water-Supply Paper 2336–A 48 p.

McNeill, J.D., 1980. Electrical Conductivity of Soils and Rocks (Technical Note TN-5, Geonics, Ltd).

Minsley, B.J., Burton, B.L., Ikard, S., Powers, M.H., 2011. Hydrogeophysical investigations at Hidden Dam, Raymond, California. JEEG 16 (4), 145–164.

Morgan, F.D., Williams, E.R., Madden, T.R., 1989. Streaming potential properties of Westerly Granite with applications. J. Geophys. Res. Solid Earth Planets 94, 12449–12461.

Revil, A., Jardani, A., 2013. The Self-Potential Method: Theory and Applications in Environmental Geosciences. Cambridge University Press.

Revil, A., Pezard, P.A., Glover, P.W.J., 1999. Streaming potential in porous media 1. Theory of the zeta potential. J. Geophys. Res. Solid Earth 104, 20021–20031.

Rose, P.R., 1972. Edwards group, surface and subsurface, Central Texas; Report of Investigations 74. Bureau of Economic Geology, Austin, Texas.

Rucker, D.F., Glaser, D.R., 2015. Standard, Random and Optimum Array Conversions from Two-pole Resistance Data. J. Environ. Eng. Geophys. 20 (3), 207–217.

Saribudak, M., 2016. Geophysical mapping of Mount Bonnell fault of Balcones fault zone and its implications on Trinity-Edwards Aquifer interconnection, Central Texas, USA. Lead. Edge 936–941.

Saribudak, M., Hauwert, N.W., 2017. Integrated geophysical investigations of Main Barton Springs, Austin, Texas, USA. J. Appl. Geophys. 138 (2017), 114–126.

Saribudak, M., Hawkins, A., Saraiva, K., Terez, J., Stoker, K., 2010. Geophysical Signature of Haby Crossing Fault and its Implication on Edwards Recharge Zone, Medina County, Texas, Contribution to the Geology of South Texas. pp. 321–328.

Saribudak, M., Hawkins, A., Stoker, K., 2012. Do air-filled caves cause high resistivity anomalies? A six-case study from the Edwards Aquifer Recharge Zone in San Antonio, Texas. Houston Geol. Soc. Bull. 54 (9), 41–49.

Saribudak, M., Hunt, B., Smith, B., 2013. Resistivity Imaging and Natural Potential Applications to the Antioch Fault Zone in the Onion Creek/Barton Springs Segment of the Edwards Aquifer: Presented at Gulf Coast Association of Geological Societies 62nd Annual Convention.

Saribudak, M., Ruder, M., Nieuwenhuise, B.V., 2018. Hockley Fault revisited: more geophysical data and new evidence on the fault location, Houston, Texas, Geophysics. Vol. 83 (3), 1–10 (May–June 2018).

Shah, S.D., Smith, B.D., Clark, A.K., Payne, J.D., 2008. An Integrated Hydrogeologic and Geophysical Investigation to Characterize the Hydrostratigraphy of the Edwards Aquifer in an Area of Northeastern Bexar County, Texas, USGS Scientific Investigations Report 2008–5181.

Small, T.A., Clark, A.K., 2000. Geologic framework and Hydrogeologic characteristics of the Edwards Aquifer outcrop, Medina County, Texas: U.S. Geological Survey Water-Resources Investigation Report 00–4195 (10 p., 1 sheet).

Small, T.A., Hanson, J.A., Hauwert, N.W., 1996. Geologic framework and hydrogeologic characteristics of the Edwards Aquifer outcrop (Barton Springs Segment), northeastern

Hays and southwestern Travis Counties. U.S. Geological Survey Water Resources Investigations 964306, Texas (15 p. Prepared in Cooperation with the BS/EACD and TWDB).
Smith, B.A., Hunt, B.B., 2010. Flow potential between stacked karst aquifers in Central Texas. Advances in Research in Karst Media. In: Andreo, B., Carrasco, F., Duran, J.J., LaMoreaux, J.W. (Eds.), 4th International Symposium on Karst, April 26–30 Malaga, Spain. Springer, pp. 43–48.
Smith, B.D., Cain, M.J., Clark, A.K., Moore, D.W., Faith, J.R., Hill, P.L., 2005. Helicopter Electromagnetic and Magnetic Survey Data and Maps, Northern Bexar County: U.S. Geological Survey Open-file Report 2005–1158.
Stein, W.G., Ozuna, G.B., 1996. Geologic framework and hydrogeologic characteristic of the Edwards Aquifer recharge zone, Bexar County, Texas. U.S. Geological Survey Water- Resources Investigation Report 95-4030, 1:75,000 Scale, 8p. 1 Plate.
Vichabian, Y., Morgan, F.D., 2002. Self potentials in cave detection. Lead. Edge 23, 866–871.
Wong, C., Kromann, J.B., Hunt, B., Smith, B., Banner, J., 2014. Investigating groundwater flow between Edwards and Trinity Aquifers in Central Texas. Groundwater 52 (4), 624–639.